THE ASTROPHYSICAL JOURNAL, 269:57–72, 1983 June 1

QUASAR EVOLUTION AND GRAVITATIONAL COLLAPSE

A. CAVALIERE,[1] E. GIALLONGO,[1] A. MESSINA,[2] AND F. VAGNETTI[1]
Received 1982 April 12; accepted 1982 November 18

ABSTRACT

The paper presents three convergent results concerning the sources in the active nuclei of quasars and radio galaxies that derive their power from conversion of gravitational energy.

We first derive, for several leading models based on liberation of gravitational energy from mass in a compact supply, the laws governing the secular change $\dot{L}$ of the primary power driving the individual sources, and identify their common and key property: $\dot{L}$ increases, and eventually decreases, linearly or faster with the power itself, so that the associated time scales $t_s = L/|\dot{L}|$ obey $dt_s(L)/dL \leq 0$.

We then describe a general statistical framework to populate with sources the (luminosity, cosmic time)-plane, based on a continuity equation that embodies a given $\dot{L}$. We show how the main features of the populations depend primarily on $\dot{L}$, while the memory of the initial details is easily erased. With $\dot{L}$ as derived above, we obtain basic evolutions of the density ($\dot{L} > 0$) and of the luminosity ($\dot{L} < 0$) type, with a global differential character.

Finally we compute the full evolution functions, comprising a brightening ($\dot{L} > 0$) and a dimming ($\dot{L} < 0$) phase, corresponding to three such models. Sub-Eddington accretion onto a massive black hole from a star cluster that self-destroys by collisions is close to reproduce the general course of the empirical models for the optical QSO population.

Subject headings: galaxies: nuclei — quasars — radio sources: galaxies

I. INTRODUCTION

A striking increase of density and/or luminosity with look-back time is exhibited by different classes of active galactic nuclei.

Steep-spectrum radio sources (mainly extended structures of radio galaxies) were the first objects recognized as a differentially evolving population (Longair 1966); more detailed information on the epoch dependence of their luminosity function is now gradually building up from various population observables (see Wall, Pearson, and Longair 1980, 1981; Peacock and Gull 1981). The flat-spectrum radio sources (mainly compact components of radio-loud quasars) appear now to have a comparable distribution (see also Kellermann and Pauliny-Toth 1981). The quasars (emitting from very compact regions) show in the optical band evidence of an even stronger evolution from V/V_m tests, from counts and from (still coarse) redshift resolutions of their luminosity function (Braccesi *et al.* 1980; Koo and Kron 1982; Schmidt and Green 1982; Setti and Woltjer 1982); a similar, or somewhat weaker, evolution in X-rays is consistent with the results of the deep and medium-sensitivity surveys by *HEAO 2* (Cavaliere *et al.* 1981; Avni and Tananbaum 1982; Maccacaro *et al.* 1982).

The data are conveniently represented in the form of populations $\rho(P, z)$ of the plane monochromatic power-redshift (cf. Peacock and Gull 1981; van der Laan and Windhorst 1982; Schmidt and Green 1982); these, within the definition allowed by persistent limits to the dynamic ranges, exhibit a number of similarities. The evolution functions $\rho(P, z)/\rho(P, 0)$ increase strongly, by a factor 10^2–10^4 to $z \sim 2$–3. Their increase, however, is differential in luminosity: it concerns mainly the bright sources, most of the transition occurring within a range of order 10 centered on a threshold: e.g., $P_{408} = 2 \times 10^{33}$ ergs s^{-1} Hz^{-1}, and a less agreed upon $M_B \sim -23$.

The evolutions are also differential in cosmic time: they reach substantial amplitude over the range $z = 0.3$–1; on the other hand, the fast convergence of the counts at the faint end severely bounds the number of weak early sources, and even the strongest ones should level off or perhaps disappear beyond $z \sim 3.5$.

The compact radio sources may constitute a subsection of the extended ones, promoted by beaming effects (Blandford and Rees 1978; Scheuer and Readhead 1979) to higher apparent powers. Gravitational lensing (Turner 1980; Peacock 1982) may alter at the bright end the counts of the very compact optical sources. It would require extreme assumptions, however, to explain all of the dependence on cosmic epoch in those terms, including in a common pattern the very compact and the very extended objects. Nor do the distribution of the external medium and the inverse Compton losses appear to affect substantially the collective behavior of the extended sources (cf. Wall and Benn 1982): some more fundamental and common driving agency is indicated.

[1] Istituto Astronomico, Università di Roma, Italy.
[2] Istituto di Astronomia, Università di Bologna, Italy.

This paper is intended to discuss how the bulk of the evolutions can be understood as an *intrinsic population dynamics* driven, model-independently up to a point, by the common gravitational nature of the primary energy source for the individual objects (see also the brief outline by Cavaliere *et al.* 1982).

II. THE ROLE OF GRAVITY

That the "prime mover" should be identified with a converter of gravitational energy associated with a massive, collapsed or collapsing object, is now a widely accepted view (cf. Rees 1978). We need to recall only briefly a direct argument: given that the energy production occurs within a size $\lesssim 10^{15}$ cm (as indicated by straight time variability, or as required by an early collimation in jet models, Rees, Begelman, and Blandford 1980), and given that many sources produce an energetics $\gtrsim 10^{60}$ ergs (as inferred from statistics; cf. Schmidt 1978; Woltjer 1978), it follows that the gravitational energy released in the very process of gathering the configuration dominates other forms of mass conversion having an efficiency bounded by $\epsilon \leq 10^{-2}$ (as typically nuclear energy) when $E_{60}/R_{15} \geq 3\epsilon_{-2}^{2}$ holds. The mass involved is, in units of $10^8\, M_\odot$, $M_8 = \eta^{-1/2}(E_{60}\, R_{15})^{1/2}$ if η is the efficiency for conversion of the gravitational energy released into the radiation observed; hence it must be close to, if not within, its gravitational horizon which has dimensions $R_H \sim 3 \times 10^{-2} R_{15}\, M_8$.

Such "gravitational engines" comprise two parts (coinciding only in particular models): the active mass in whose potential the energy is liberated, and a mass supply providing the fuel to the former. Accretion of gas from a whole galactic body may fuel some low-level activity, drifting over galactic lifetimes. Large sustained fueling rates, as required to power radiative outputs $\gtrsim 10^{45}$ ergs s^{-1} for $\approx 10^8$ yr, obtain from a local mass supply ($M \gtrsim 10^8\, M_\odot$ within $R \lesssim 1$ pc) held in a quasi-equilibrium compact configuration against self-gravity by a dynamical constraint—viz., angular momentum or orbital kinetic energy. Only to the extent that the constraint is released or dissipated can the collapse proceed, and more mass is supplied to the inner engine where more energy is eventually liberated.

Many specific models (discussed in the Appendix) fit in this heuristic scheme; each one focuses on a prevailing constraint and one dominant dissipation process, setting accordingly an initial time scale $t_s \approx 10^9$ yr for the activity. The bulk of the subsequent course may be anticipated on the basis of the dynamics of the mass supply: as the constraint is dissipated, the configuration contracts under self-gravitation and/or the central active mass grows larger, to the effect that the rate of constraint dissipation generally increases and so does the power output L; but the increase of L may be restrained by imperfect coupling of the inner engine to the mass supply, or by limits to growth of the central mass. Two general outcomes will result. First, the primary source will brighten ($\dot{L} > 0$) at a rate depending only on the power L itself; this is because for a closed system the local gravity alone determines both L and $\dot{L}$, or equivalently, L rather than the cosmic time of the outside universe labels the evolutionary stages. Second, as L increases, the effective time scale $t_s = L/\dot{L}$ will decrease from its initial value (implying $\ddot{L} > 0$), since the driving self-gravity dominates the rate of loss of the braking constraint with its accelerating, nonlinear trend that becomes irresistible at strong field values.

The second outcome will hold true, however, only up to the point when about half of the mass stockpiled has been used up—for instance, by having crossed the event horizon. Thereafter, either because the central black hole cannot grow substantially larger, or because the mass supply is no longer self-gravitating, the constraint dissipation rate saturates or decreases, and the release of gravitational power will decrease; thus the radiation observed must exhibit a progressive dimming ($\dot{L} < 0$) comprising roughly half of the energy emitted, with $L/|\dot{L}|$ increasing as the stockpile is gradually exhausted.

III. MODES OF ENERGY RELEASE

In the Appendix, we check the extent to which the above surmises are verified in various classes of models that have been proposed to describe the processes of liberation of gravitational energy. By the same token, we derive the specific laws for the secular change of the power production. The results are collected in Table 1.

The general conclusion from this set of models is that for a compact mass supply the rate of change of gravitational power $\dot{L}$ is indeed expressed in terms of L itself:

$$\dot{L} = f(L)\,. \tag{3.1}$$

In fact, most models in this line end up in expressions for $\dot{L}$ of the more specific *scale-free* and power-law form:

$$\dot{L} = \pm A L^{1+p} \tag{3.2}$$

with $0 < p \lesssim 1$; $\dot{L} > 0$ describes the "brightening" phase and $\dot{L} < 0$ the "dimming" phase. These expressions integrate to

$$L = L_0 \left[1 - \frac{\Delta t}{\tau_0}\right]^{-1/p} \qquad \text{with} \qquad \tau_0 = \frac{1}{pAL_0{}^p}\,; \tag{3.3}$$

the instantaneous time scale is given by $t_s = L/|\dot{L}| = p|\tau_0|(L_0/L)^p$.

TABLE 1

SECULAR CHANGE OF THE PRIMARY POWER OUTPUT FOR MODELS RELYING ON A COMPACT MASS SUPPLY

Mode of Energy Release	Constraint	$\dot{L} = f(L)$	$t_s = L/\dot{L} \times 10^9$ yr
Class 1: Accretion onto a Black Hole: $L = \eta \dot{M} c^2$			
Black hole accreting from a star cluster, sub-Eddington regime (brightening)	v^2, dissipated via tidal disruption and cooling	AL^{1+p}, $p = 0.25$	$\frac{R_{ipc}}{N_{i8}} \frac{N_{i8}^{1/2}}{m_{i6}^{1/3}}$
Black hole accreting from a dense star cluster: Super-Eddington regime (brightening)	v^2, dissipated via disruptive collisions and cooling	$a(\Lambda - L)^{-k}$, $1 \leq k \leq 4.5$	$\frac{L_i}{\Lambda}\left(\frac{R_{ipc}}{N_{i8}}\right)^{7/2} N_{i8}^2$
Sub-Eddington regime (brightening)	Same as above	AL^{1+p}, $1.22 \lesssim p < 2$	$\left(\frac{R_{ipc}}{N_{i8}}\right)^{7/2} N_{i8}^2$
Dimming	star dynamics determined by the black hole	$-AL^{1+p}$, $p = 0.5$	$\left(\frac{R_{ipc}}{N_{i8}}\right)^{7/4} \frac{R_{ipc}^{7/4} N_{i8}^{1/2}}{m_8^{1/4}}$
Class 2: Rotating Magnetized Configurations: $L = cR_c^2 B_p^2$			
Spinar, spun up by contraction: Brightening	J, removed via $B_\perp$ electrodynamically	AL^{1+p}, $0.75 \leq p < 1$	$0.1\left(\frac{GM^2}{\phi^2}\right)^{1/4} \frac{M_8}{L_{42}^{3/4}}$
Dimming	$\boldsymbol{B}$ aligns to $\boldsymbol{J}$	$-AL^{1+p}$, $p = 0$	$\frac{t_{s+}}{\cos^2 \chi_i}$
Class 3: Accretion and Rotation Combined: $L = cR_c^2 B_p^2$			
Magnetized accretion disk fed by a star cluster	v^2, dissipated via tidal disruption; and J, electrodynamically	AL^{1+p}, $p \sim 0.1$	$m_8^{-1/3}$

The other explicit type $\dot{L} = a(\Lambda - L)^{-k}$ (with $a > 0$ and $L \lesssim \Lambda/2$) where a *scale* $L_{\mathrm{E\,max}}$ appears, integrates to

$$L = \Lambda - (\Lambda - L_0)\left[1 - \frac{\Delta t}{\tau_0}\right]^{1/(k+1)} \quad \text{with} \quad \tau_0 = \frac{(\Lambda - L_0)^{k+1}}{a(k+1)}\,; \tag{3.4}$$

in this case $t_s = L/\dot{L} = (k+1)\tau_0 L(\Lambda - L)^k/(\Lambda - L_0)^{k+1}$ obtains.

In all instances $d|f|/dL > 0$ holds. But in many cases (cf. eqs. [A1], [A4], [A5], [A6], [A8]) the dependence of $f(L) \propto L^{1+p}$ $(p > 0)$ is more than linear, so that $|f(L)|/L$ also increases with L; that is, the time scale $t_s = L/|\dot{L}|$ shortens continuously with L increasing; and this will be a crucial feature for the brightening as well as for the dimming phase. The index for this behavior is $p = -d \ln t_s/d \ln L$, which generalizes the exponent p appearing explicitly when $f(L) \propto L^{1+p}$ holds.[3]

The modes of energy release mark in turn the source statistics with a recognizable imprint through their secular behavior and the associated time scales.

IV. THE STATISTICAL FRAMEWORK

The basic link of the population dynamics with the individual object's time scales is provided (as pointed out by Cavaliere, Morrison, and Wood 1971, CMW) by the conservation law

$$\frac{\partial N}{\partial t} + \frac{\partial}{\partial L}(\dot{L}N) = S(L, t) \tag{4.1}$$

for $N(L, t)$, the comoving density of sources per unit total luminosity interval at the cosmic epoch t, or equivalently the epoch-dependent luminosity function. This continuity equation relates the *gradients* $\partial N/\partial t$, $\partial N/\partial L$ by means of two input functions, $\dot{L}(L, t)$ and $S(L, t)$.

Of prime importance is $\dot{L}$, the same function that describes the secular rate of change of the single sources, discussed in §§ II and III; in fact, the curves in the (L, t)-plane defined by the equation $dL/dt = \dot{L}(L, t)$ are the characteristics of the partial differential equation (4.1). They guide, as it were, the propagation of $N(L, t)$ at successive times over the L coordinate and thus determine the associated reshaping of the luminosity function.

[3] Note that the total energetics, given by $E(L) = \int^L L dL'/f(L')$ and approximated by $E \approx t_s L \propto L^{1-p}$, grows but weakly with L_{max} increasing when $0 < p < 1$ holds.

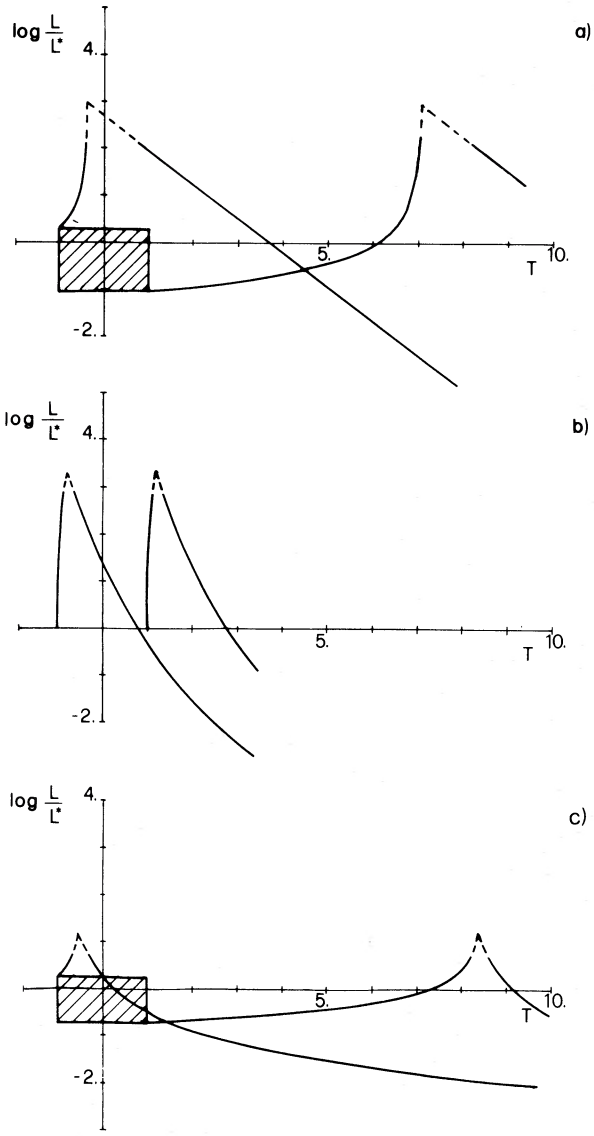

FIG. 1.—Characteristics. (*a*) Brightening with divergence, $\dot{L} = AL^{1+p_+} > 0$, $D > 0$; switching over at $L = L_{max}$ to neutral dimming, $\dot{L} = -AL < 0$, $D = 0$. The parameter values are: $\tau_+(L^*) = \delta t/2$, $p_+ = 0.75$; and $\tau_-(L^*) = 0.3\delta t$, $p_- = 0$. The location of the birth function $S(L, t) \neq 0$ is marked by the shaded area, centered at $t = t^*$ with full width δt. Here and in the following, $T = 2(t - t^*)/\delta t$. (*b*) Brightening with convergence $\dot{L} = a(\Lambda - L)^{-k} > 0$, $D < 0$; switching over at $L_{max} = \text{const}$ to dimming with convergence $\dot{L} = -AL^{1+p_-} < 0$, $D < 0$. Parameters: $\tau_+(L^*) = \delta t/2$, $k = 4.5$; $\tau_-(L^*) = 3\delta t/2$, and $p_- = 0.5$. (*c*) Brightening with divergence $\dot{L} = AL^{1+p_+} > 0$, $D > 0$; switching over at $L_{max} = \text{const}$ to dimming with convergence $\dot{L} = -AL^{1+p_-} < 0$, $D < 0$. Parameters: $\tau_+(L^*) = \delta t/2$, $p_+ = 1.2$; $\tau_-(L^*) = \delta t/2$, $p_- = 0.5$.

We concentrate here on characteristics of the form $\dot{L} = f(L)$.[4] Crucial to the change of $N(L, t)$ is their relative convergence or divergence in a (log L, t)-plot; the discriminating quantity (at some variance with CMW) is based on the index $p = -d \ln t_s/d \ln L$:

$$D \equiv p \text{ sign } \dot{L} \begin{cases} >0 \text{ for divergence} \\ <0 \text{ for convergence} . \end{cases} \tag{4.2}$$

The value of D is obvious when $\dot{L} = \pm AL^{p+1}$ holds. When $\dot{L} = a(\Lambda - L)^{-k}$ instead applies, the corresponding value of D is given by $D = [kL/(\Lambda - L) - 1]$ sign $\dot{L}$; this describes a mixed behavior: $D < 0$ (convergence) up to $L = \Lambda/(k + 1) = 2\Lambda/(11 + 7\beta)$, and divergence upward of this value; since in this model $L \lesssim \Lambda/2$ holds, a diverging section obtains only for $\beta \to 0$. See Figure 1.

[4] Most results to follow hold also for the separable form $\dot{L} = f(L)\phi(t)$ (the external world affects equally all powers L), with the rescalings $dt' = dt\phi(t)$ and $S' = S/\phi(t)$.

Divergence of the characteristics implies a "rarefaction" of $N(L, t)$ with increasing t, and convergence implies a "condensation": mathematically intuitive (note that eq. [4.1] writes $dN/Ndt = \partial\dot{L}/\partial L$ where $S = 0$ holds), these properties are fully illustrated in their astrophysical implications in §§ V and VI. To anticipate an example, diverging characteristics imply a broadening of the luminosity function, in fact a spread upward for a brightening phase with divergence. Circumstances of this sort alleviate the demands on $S(L, t)$, the second input function in equation (4.1).

The birth function $S(L, t)$ describes the appearance of new objects in some region δL, δt of the (L, t)-plane. These are then propagated along the characteristics as described by the explicit solution of equation (4.1):

$$N(L, t) = \frac{1}{f(L)} \int_{\delta t} dt' S(L', t') f(L') \; ; \tag{4.3}$$

$L' = L'(t'; L, t)$ is taken along the characteristic joining the points L', t' with L, t, of which equations (3.3) and (3.4) give explicit expressions.

As the formation process is still under debate (see Appendix), two extreme cases are considered. $S(L, t) \neq 0$ may be confined to the smallest possible ranges δL, δt. For example, if the beginning of the nuclear activity is related to protogalactic era, $\delta t \lesssim t \ll H_0^{-1}$ is an obvious choice; a hypothetical continuous growth of black holes from seeds of stellar-type masses would require only a very small $\delta L \approx L \approx 10^{40}$ ergs s^{-1}. Here S plays the role of an initial synchronizer: like so many other cosmic events (Layzer 1976), also the population evolutions would be started by, and coordinated to, the cosmic evolution through an initial condition. The solution (4.3) rapidly loses the memory of the initial details, as the spread of N over the (L, t)-plane is soon redirected by the distribution of the time scales $t_s(L) = L/|\dot{L}|$ in the way described above.

At the opposite extreme, $S(L, t)$ may still be producing new objects here and now, under continued control of large-scale conditions; correspondingly, the luminosity functions will depend substantially on the formation process.

V. MODES OF EVOLUTION

Here we examine in some detail the basic solutions of which the full evolution is composed, considering first the regions of the (L, t)-plane where $S(L, t) = 0$ holds, and then those within or near δL, δt where the influence of S is substantial.

a) Brightening Phase, Rarefaction: $\dot{L} > 0$, $D > 0$

Taking up the discussion by CMW, when $\dot{L} = AL^{p+1}$ holds, the solution reads

$$N(L, t) = (L_0/L)^{p+1} N_0[L_0(L, t)] \, , \tag{5.1}$$

where $N_0(L_0)$ is the initial luminosity distribution and $L_0(L, t)$ is obtained by inverting equation (3.3).

After equation (5.1), consecutive ranges of decreasing L_0 in the initial distribution $N_0(L_0)$ evolve in succession; the ensuing development of $N(L, t)$ may be associated with three well recognizable regions of the L, t plane:

i) In the region at low L defined by $\Delta t \ll \tau(L)$ no evolution takes place, so that $N(L) \sim N_0(L_0)$.

ii) In the region at high L and early Δt some evolution in luminosity begins from the initial $N_0(L_0)$ toward the asymptotic form $N(L) \propto 1/L^{1+p}$ (see Fig. 2).

iii) In the region at high L and late t defined by $t > \tau(L)$, i.e., $L^p > 1/pAt$, fast evolution takes place. Equation (5.1) reduces to the form

$$N(L, t) \to N(L) g(t) \begin{cases} N(L) \sim 1/L^{1+p} \, , \\ g(t) = t^{-(1+p)/p} N_0[(1/t)^{1/p}] \end{cases} \tag{5.2}$$

factorized into a density function $g(t)$, and a self-similar luminosity function $N(L) \propto 1/L^{1+p}$. The latter results from a steady balance between inflow of objects into this region and outflow toward such high luminosities that $\tau(L) \ll t$ holds, and is independent of the initial shape $N_0(L_0)$, whereas $g(t)$ does depend on $N_0(L_0)$. The result is a *differential density evolution.* See Figure 2.

For example, if $N_0(L_0)$ peaks at L_u, say, with a rise $N_0 \propto L_0^{\alpha}$ and a decline $N_0 \propto L_0^{-\mu}$ ($\mu > 2$ is required for convergence), then the explicit behavior of $g(t)$ is $g(t) \propto t^{-(1+p+\alpha)/p}$; this power-law density evolution, however, tends to level off at such early times that $\Delta t < \tau(L)$ is satisfied for the relevant L's, and it may even have a maximum at $\Delta t = \tau(L_u)\{[\mu/(1 + p + \alpha)] - 1\}^p$ if $\mu \geq 1 + p + \alpha$ (CMW). It is easy to check that the evolutionary factor $g(t)$ just reflects the distribution of the initial lifetimes at low luminosities: since lifetime and luminosity are related by $\tau_0 \propto L_0^{-p}$, an initial shape $N_0(L_0) \propto L_0^{\alpha}$ corresponds to $N(\tau_0) \propto \tau_0^{-(1+p+\alpha)/p}$.

On the other hand, the "initial" distribution $N_0(L_0)$ may be reinterpreted as one produced by a birth function confined to still earlier times; a simple example is provided by a birth function concentrated at a single luminosity L^*, that is, $S(L, t) = \delta(L - L^*)k(t)$:

$$N(L, t) = \int_{t_1}^{t_2} dt' \delta(L' - L^*) k(t') \frac{f(L)}{f(L)} = \frac{1}{f(L)} \, k[t^*(L^*; L, t)] \, , \tag{5.3}$$

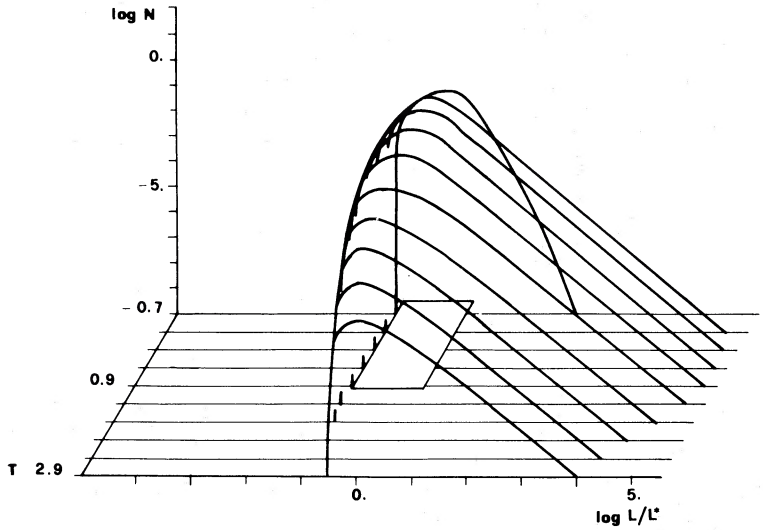

FIG. 2.—Mode of evolution: $N(L, t)$ (here and in the following, normalization $S_{max} = 1$) that corresponds to brightening with divergence, from a birth function $S \propto [1 - b^2(L/L^* - 1)^2](1 - T^2)$. Parameters: $\tau(L^*) = \delta t$, $p = 0.75$. Note the gradual steepening of $N(L)$ into the self-similar shape $\propto L^{-(1+p)}$ and the strong density evolution.

where t^* corresponds to L^* on the characteristic passing through L, t. When $f(L) = AL^{1+p}$, t^* may be expressed as

$$t^* = t - (\tau^* - \tau) \equiv t - \left(\frac{1}{pAL^{*p}} - \frac{1}{pAL^p}\right).$$

Thus

$$N(L, t) = \begin{cases} \dfrac{1}{AL^{p+1}}\, k(t - \Delta\tau) & \left(L^* \le L_{low} \le L \le L_{up} \le \dfrac{L^*}{[1 - (t - t^*)/\tau^*]^{1/p}}\right) \\ 0 & \text{(outside)}. \end{cases} \tag{5.4}$$

We shall consider birth functions $S(L, t) = (3/4T)\delta(L - L^*)(1 - T^2)$ with $T = 2(t - t^*)/\delta t$ that begin at a definite time $t = t^* - \delta t/2$, say; reach a maximum rate at $t = t^*$; and vanish at $t = t^* + \delta t/2$, with a parabolic behavior: the simplest scheme for a smooth birth rate evenly spread over δt. The result is

$$N(L, t) = \frac{3p\tau^*}{2\delta t L^*} \frac{1 - \{T - 2(\tau^*/\delta t)[1 - (L^*/L)^p]\}^2}{(L/L^*)^{p+1}} \quad (\text{when } \neq 0). \tag{5.5}$$

Figure 2 shows the evolution from a more complex $S(L, t) \propto [1 - b^2(L/L^* - 1)^2][1 - T^2]$, with a finite spread also in luminosity.

b) Brightening Phase, Condensation: $\dot{L} > 0$, $D < 0$

The specific case $\dot{L} = a(\Lambda - L)^{-k}$ yields

$$N(L, t) = \left[\frac{\Lambda - L_0(L)}{\Lambda - L}\right]^k N_0[L_0(L)]. \tag{5.6}$$

$L_0(L, t)$ is given by equation (3.4). The result is shown in Figure 3: the average L increases while the range ΔL shrinks.

c) Dimming Phase, Condensation or Neutral Behavior: $\dot{L} < 0$, $D \le 0$

The set of cases $\dot{L} = -AL^{p+1}$ has some analogy with the behavior in energy and time of a population of particles undergoing radiative energy losses; cf., e.g., Kardashev (1962).

The case $D = 0$ (i.e., $p = 0$, $\dot{L} = -AL$) is quite simple: on a (log L, t)-representation $N(L)$, once formed, displaces toward lower values of L without changing shape; this corresponds to a *uniform luminosity evolution*; see, e.g., the dimming section of Figure 5.

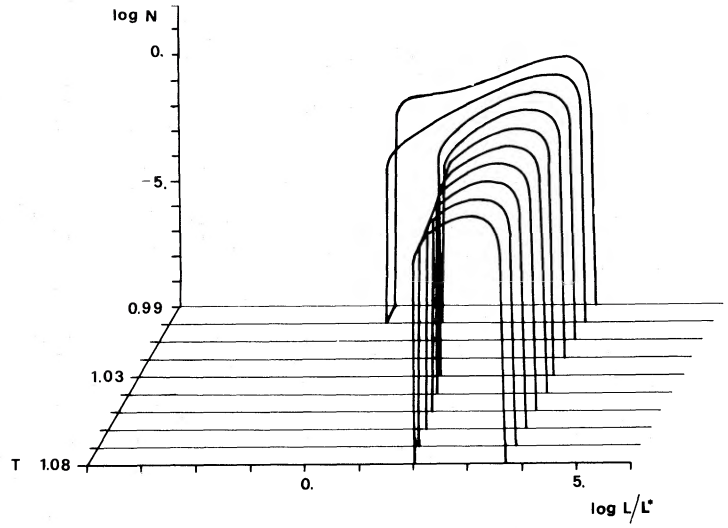

FIG. 3.—Mode of evolution: brightening with convergence, from a birth function $S \propto \delta(L - L^*)(1 - T^2)$: $\tau(L^*) = 7.5\delta t$, $k = 4.5$

Consider now the cases $D < 0$ ($p > 0$). Given an initial ($t = 0$) broad distribution declining like $N_0(L_0) = kL_0^{-\gamma}$ ($\gamma < 1 + p$), the later distributions follow a *differential luminosity evolution*:

$$\begin{aligned} N(L, t) &= kL^{-\gamma}[1 - pAL^p t]^{(\gamma - p - 1)/p} \\ &\to kL^{-\gamma} \quad [L < (1/ptA)^{1/p}] \\ &= 0 \qquad [L > (1/ptA)^{1/p}] . \end{aligned} \tag{5.7}$$

In real life the cutoff is substituted by a break when a distribution of constitutive parameters is considered; for example, $f(A) \propto A^a$ ($a > -1$ for convergence):

$$\bar{N}(L, t) \to kh \frac{L^{-\gamma - p(a+1)}}{(pt)^{a+1}} \quad L > \left(\frac{1}{ptA_{\max}}\right)^{1/p} \tag{5.8}$$

with

$$h \equiv \int_0^1 dx\, x^a (1 - x)^{[\gamma - (p+1)]/p} .$$

The faint end displaces downwards following the characteristic: $L_{\min} = (ptA)^{-1/p}$.

If new objects are produced at a constant rate with some broad L-distribution: $S(L, t) = kL^{-\gamma}$ ($\gamma < 1 + q$), then the resulting $N(L, t)$ exhibits a break, even for identical objects (cf. Fig. 4)

$$\begin{aligned} N(L, t) &= \frac{kL^{-(\gamma + p)}}{A(\gamma - 1)}[1 - (1 - pAL^p t)^{(\gamma - 1)/p}] \\ &\to kL^{-\gamma} t \qquad [L < (1/pAt)^{1/p}] \\ &\to \frac{kL^{-(\gamma + p)}}{A(\gamma - 1)} \quad [L > (1/pAt)^{1/p}] . \end{aligned} \tag{5.9}$$

If instead γ is large and the range δL comparatively small, the slope breaks from $-\gamma$ to $-(p + 1)$ toward low L's. The relevance of such boundary conditions is explained below.

d) Brightening and Dimming Coupled

The full course of the individual luminosity change will comprise a brightening and a dimming phase. We shall denote by $N_+(L, t)$ the population of the brightening objects, and by $N_-(L, t)$ that of the dimming ones; the total

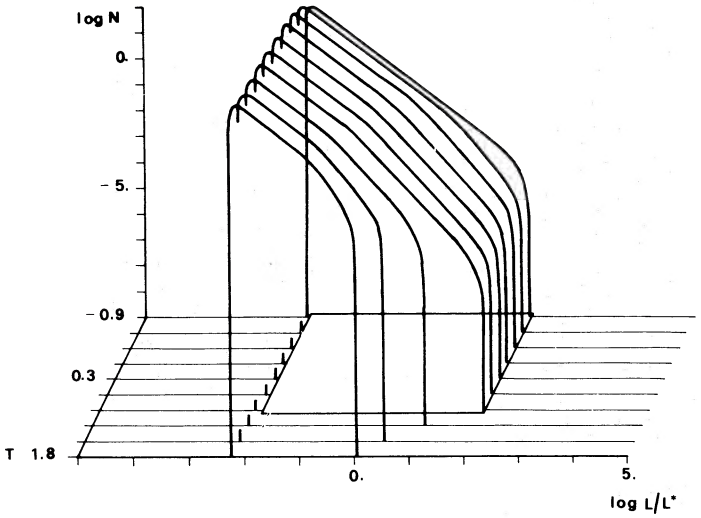

FIG. 4.—Mode of evolution: dimming with convergence from a birth function constant over the time δt, with $S(L) \sim L^{-\gamma}$, $\gamma = 1.6$, $\tau(L^*) = \delta t/2$, $p = 0.5$. Note the luminosity evolution; the behavior is described schematically by eqs. (5.7) and (5.9). If the last time represented is taken as the present epoch, $S(t)$ is active over a considerable fraction of H_0^{-1}.

population will be $N(L, t) = N_+(L, t) + N_-(L, t)$. At the maximum values of L for the brightening phase, $N_+(L, t)$ gives rise to an effective birth function for $N_-(L, t)$. The general coupling of N_- with N_+ is described by:

$$\frac{\partial N_+}{\partial t} + \frac{\partial}{\partial L}(\dot{L}_+ N_+) = S - S_- ,$$
$$\frac{\partial N_-}{\partial t} + \frac{\partial}{\partial L}(\dot{L}_- N_-) = S_- , \tag{5.10}$$

where $S_-(L, t)$ is a number-conserving functional of N_+.

When the spread in the values of L_{max} (from a given model) is large, a "statistical" coupling may provide a realistic representation:

$$S_-(L, t) = N_+(L, t)/t_r(L) . \tag{5.11}$$

Here $t_r^{-1}(L)$ is an increasing function of L that describes the increasing probability for an object to switch over to its dimming phase. This form of coupling is used in Figure 5.

When instead the maximum luminosity L_{max} is reasonably well defined, it is convenient to impose directly as a boundary condition the flux conservation at $L = L_{max}$:

$$N_-(L_{max}, t)\frac{dL_-}{dt} + N_+(L_{max}, t)\frac{dL_+}{dt} = 0 \tag{5.12}$$

with $dL_\pm/dt = f_\pm(L_{max}) - dL_{max}/dt$.

If instead the model fixes the brightening range, the values of L_{max} are proportional to the initial luminosities L_0; then the flux conservation applies to the differential subset of objects switching over at any given $L_{max} = QL_0$. This important case is represented in Figure 7. Figure 8 specifically illustrates how N_+ affects N_-. Denoting with an asterisk the central values of τ, the ratio $N_-(L_{max})/N_+(L_{max})$ is given by $p_-\tau_-^*(L_{max}/L^*)^{p_+ - p_-}/p_+\tau_+^*$ in cases of power-law $f(L)$. Dominance of N_+ over N_- is favored only when $\tau_+^* \gg \tau_-^*$ and $L_{max}/L^* \sim 1$ hold, or else when $p_+ < p_-$; in these cases $N(L)$ at intermediate times exhibits a local minimum followed by a local maximum near the bright end. Otherwise and more commonly (as represented in Figs. 7 and 8), $N_- > N_+$ holds, and $N(L)$ is monotonic at intermediate times. The rapidly decreasing $N_+ \propto L^{-(1+p_+)}$ feeds and sustains the bright end of N_- until the former disappears; thereafter, the bright end of N begins to recede for times that may well exceed δt, evolving toward the local shape. The overall result at intermediate to late times is a *luminosity evolution* somewhat L-dependent at the bright end.

Armed with this background, we can set in a perspective the results for the three models computed in full and represented in Figures 5, 6, and 7.

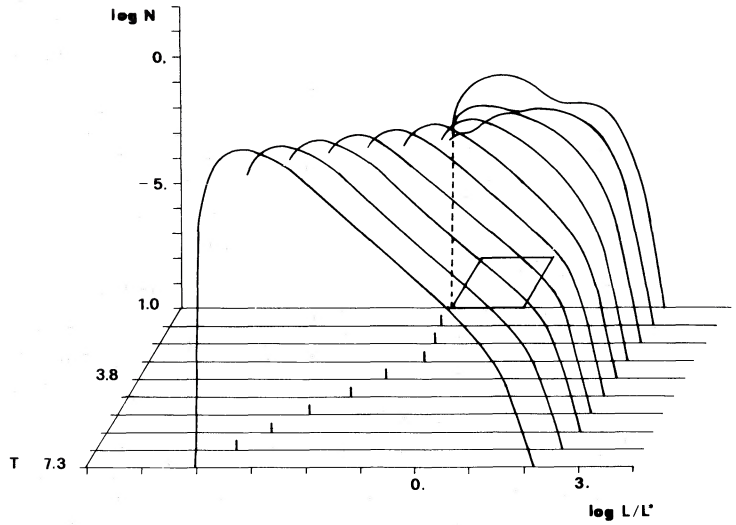

FIG. 5.—An instance of combined evolution (CE): the population $N(L, t)$ of primary sources brightening with divergence and dimming with neutral flow as in Fig. 1*a*; the birth function is $S \propto [1 - b^2(L/L^* - 1)]^2[1 - T^2]$ with $b = 1.1$. The coupling is statistical, with $t_r^{-1} = \bar{t}_r^{-1}(\bar{L}/L - 1)^{1.5}$, $\bar{t}_r = 0.01\delta t$, and $\bar{L} = 40L^*$. This case incorporates many features of the mode of energy release by spinars; but more generally, it illustrates the uniform luminosity evolution corresponding to $p_- = 0$. If the last time is taken as the present epoch, then $\delta t \approx 0.1H_0^{-1}$.

VI. DISCUSSION AND CONCLUSIONS

Here we shall concentrate on the overall aspects of our results. We use as reference terms the free-form representations of the radio data by Peacock and Gull 1981 (especially their more consistent model 4, Danese, De Zotti, and Mandolesi 1982), the data of van der Laan and Windhorst (1982), and the analysis of optical data by Schmidt and Green (1982) tempered by that of Cheney and Rowan-Robinson (1981).

A direct comparison with the data of $N(L, t)$, the epoch-dependent statistics of the power L delivered at the nucleus, requires assuming the dominant radiative emission of these sources to be proportional to L. Here we adopt the assumption as a reasonable first approximation, considering that the terminal output of L has to be radiative in the very compact sources; and considering for the extended radio sources how directly the radio volumes appear to be

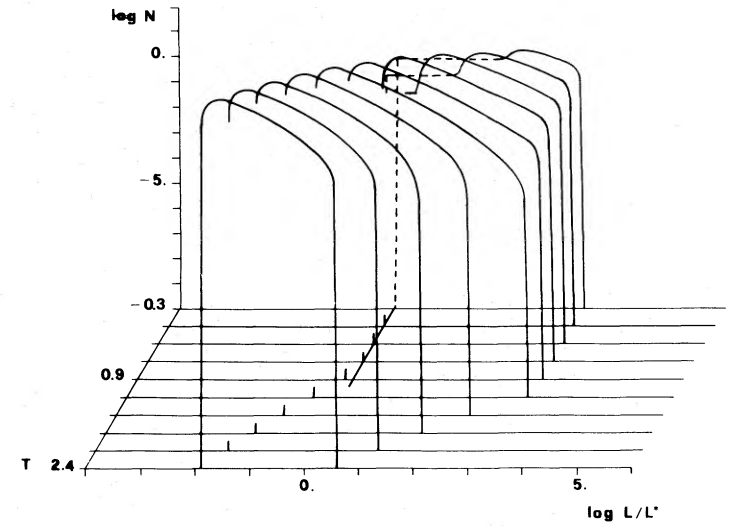

FIG. 6.—CE: brightening with convergence and dimming with convergence as in Fig. 1*b*. Birth function $S \propto \delta(L - L^*)(1 - T^2)$. Coupling after eq. (5.11) with $L_{max} = 2500L_0$. $S(L, t)$ as in Fig. 1*b*. This case incorporates many features of the mode of energy release by super-Eddington accretion onto a black hole from a collisional star cluster. Note how the range ΔL narrows, due to double convergence, shortly after $S(t)$ has died out.

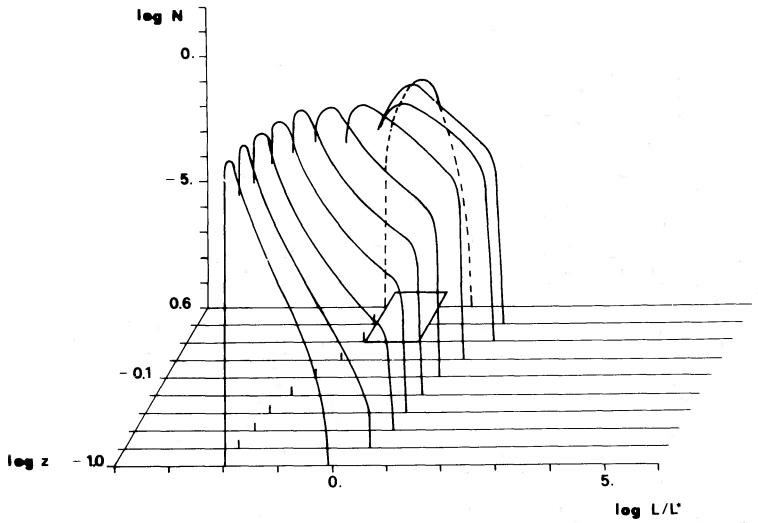

FIG. 7.—CE: brightening with divergence, and dimming with convergence as in Fig. 1*c*. Birth function $S \propto [1 + \cos B(L/L^* - 1)][1 - T^2]$ with $B = 3.9$. Coupling after eq. (5.11). The case presented here incorporates many features of the energy release by sub-Eddington accretion onto a black hole from a collisional star cluster; it is a limiting case in the following respects: $\beta \to 0$ (implying $L_{max}/L_0 \to 23$ and $p_+ \to 1.22$), and $p_- \to 0.5$. Here again $S(t)$ is active over $\approx 0.1 H_0^{-1}$.

fed by the nuclear jets (cf. Perola 1981). We also adopt as a fair indicator of the primary power the (integrated) radio emission for the radio galaxies, and the optical emission[5] for the quasars.

We stress first how our basic evolutionary modes are related to the extreme patterns of density or luminosity evolutions. When $|f(L)|$ increases more than linearly with L, the effect of a brightening phase with diverging characteristics is not only to increase the average L, but also to stretch out the luminosity function to a very broad range ΔL, even starting from objects born at low L in a very restricted range. In fact, for power-law $f(L)$, this phase ends up in a self-similar $N(L) \propto L^{-(1+p_+)}$. So the population rapidly loses memory of the initial luminosity function, and evolves in the manner of a *differential density evolution* at high L, in the region defined by $L > (1/p_+ At)^{1/p_+}$, or more generally by $t_s(L) < t$. During a dimming phase with convergence, $L \to (1/p_- At)^{1/p_-}$, the initial $N(L)$ displaces downward; it also shrinks in range, developing a cutoff (but in reality a break; cf. eq. [5.8]) at the bright end $(L > 1/pAt)^{1/p_-}$, or more generally for L such that $t_s(L) < t$ holds. The result is a marked character of *luminosity evolution, differentially* stronger near the bright end. A *uniform luminosity evolution* corresponds to a dimming with neutral characteristics, $L \propto e^{-At}$: $N(L)$ is displaced toward lower luminosities.

Luminosity evolutions require a birth function with a broad range extending up to the highest values of L. An effective birth function of this kind may be provided in a natural way by the very N_+ produced during an earlier brightening phase with divergence, characterized, e.g., by $L_{max}/L_0 \gtrsim 10$ and $\dot{L} \propto L^{1+p_+}$ with $p_+ \sim 1$. This combination of an early brightening with a later dimming phase [combined evolution (CE)] has remarkable outcomes. One specific, but representative, instance is presented in Figure 7; it matches the general course of the populations, as derived from the data with the help of the classic parametric or free-form analytical continuations (referenced to at the beginning of this section) in several respects: the early luminosity functions displaced toward, and peaking at, high luminosities; the rapid decline (driven by the decline of N_+) from $z \sim 1$ to $z \sim 0.1$ toward the local luminosity function which then changes more gradually; the magnitude of the slopes of the luminosity functions: $N(L) \propto L^{-(1+p)}$ and steeper; the slope of the counts at the bright end: $N(>F) \propto F^{-2}$ ($q_0 = 0$, or steeper depending somewhat on the parameters p_+ and τ_+) in keeping with the nature of the underlying model more apt to describe the primary source for the *optical* activity of QSOs. The counts bend subsequently and converge rapidly.

Observationally, the sharp bending of the counts (cf. Koo and Kron 1982; Setti and Woltjer 1982) requires little or no excess of weak sources at early times. The constraint is satisfied by pure luminosity evolutions (Mathez 1978; Cheney and Rowan-Robinson 1981; see also Fig. 5); but it may be appreciated from Figure 8, and we plan to show in detail, that the constraint is easily satisfied also by a CE including a brightening phase, at least when $S(L, t)$ is located at L, $\delta L > 10^{-3} L_{max}$ (otherwise, the number conservation $N\delta L = \text{const}$ might imply too high values of N at low fluxes).

[5] A reasonable body of observations now bound the infrared emission to values generally, though not always, not much exceeding the optical ones (cf. Neugebauer *et al.* 1979). As for the X-ray emission with its generally flatter spectra, direct information on the upper cutoffs is badly needed. From consideration of the X-ray background, it appears that whether the QSOs are only minor contributors to the X-ray background beyond a few keV, or major contributors (in that case their X-ray spectrum cannot exceed much beyond ~ 100 keV), in "typical" radio-quiet distant QSOs the ratio L_x/L_o would not exceed 1 by much (Cavaliere *et al.* 1981).

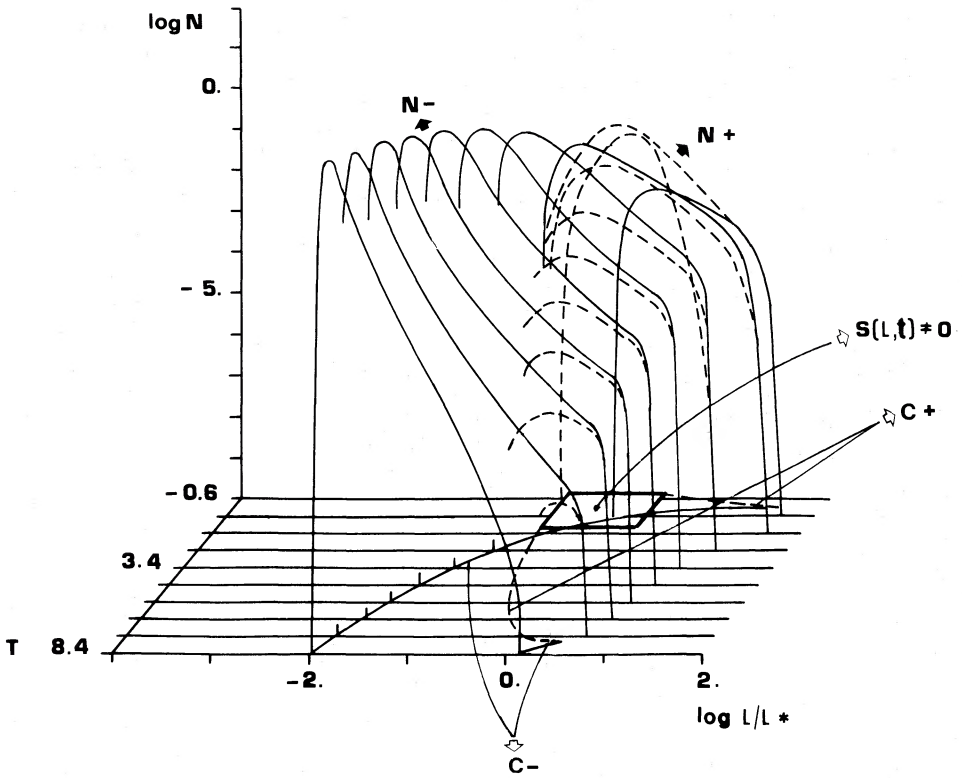

FIG. 8.—Same as Fig. 7, to illustrate the interplay of N_+ and N_- described in § V. C_+ and C_- denote the characteristics for the brightening and the dimming phase, respectively. Note that at intermediate and late epochs the population N_- (which behaves in the manner of a luminosity evolution) will be preferentially observed; N_+ provides an effective birth function of objects that begin their dimming phase. The slopes of $N_-(L)$ may be judged by comparison with $N_+ \propto L^{-(1+p_+)}$.

Two other properties of CE are worth stressing. The interplay of N_+ and N_- gives to $N(L, t)$ in the more directly observable region of the (L, t)-plane an overall character of *luminosity evolution*, faster at high L and at intermediate z. The differential details of $S(L, t)$ are largely erased during the early divergent brightening.

Alternatively to CE, one has to assume a birth of objects switched on directly at high L out to $L = L_{\max}$ (i.e., without precursor emission of the same kind, quasar-like or radio) which then undergo a pure dimming (DE). In Figure 4 we represent the case of a long-lived birth function with a broad $S(L)$: the bulk of the evolution occurs after $S(t)$ is switched off, but with $p = 0.5$ (as in the previous instance of CE) it implies a fast shrinking of $N(L)$. An early evolution obtains if either $S(t)$ is confined to the distant past, and the dimming is slower, $p < 0.5$; or when $S(t)$ itself decreases steeply, e.g., $S(t) \propto t^{-3}$. Then the populations bear clear imprints of the details of their formation process, a feature that might be variously regarded either as dynamically dull, or as highly informative on the formation stage.

The birth region can be detected from the data by checking how far into the past the gradients are related by $\partial N/\partial t = -\partial/\partial L(\dot{L}N)$; or even deriving the possible number increase $S(L, t) = \partial N/\partial t + \partial(\dot{L}N)/\partial L$, for given basic forms of L. Note, however, that in CE one will find, looking back from local conditions, an effective birth function for $N = N_+ + N_-$ beginning at intermediate epochs and extending from the bright end.

Before using the present scheme for specific and detailed fits of population observables to the optical or to the radio data, we plan to complete it with the specific K-corrections (where necessary) and with the distributions of the spectral indices. Further broadening and smoothing of the luminosity functions will be introduced by convolving in systematically the statistical distributions of the objects' constitutive parameters, as preliminarly sketched in § V, so the cutoffs appearing at the bright ends of, e.g., Figures 6, 7, and 8 will be replaced by high-luminosity tails as computed in equation (5.8) or as described by equation (5.11) and illustrated in Figure 5. The slope of the counts, however, will be little affected by tails steeper than L^{-3}. The following additions should also be considered. As for the steep-spectrum radio sources, at low powers the truly epoch-dependent action of the inverse Compton losses and that of the complex history of the confining medium will affect the early-to-intermediate evolution. For the compact sources, on the other hand, gravitational lensing may affect the bright ends.

Finally, the statistical framework designed in § IV can and will be used to derive and compare the populations corresponding to other classes of models for the energy source. The Kerr holes mentioned in the Appendix, Class 3, constitute a set of extreme compact models specifically apt to describe the energetic radio galaxies. Rapidly spun

up by the accreted mass, they undergo further brightening driven by accretion, and eventually a prolonged dimming close to a pure luminosity evolution when the accretion tapers off to the level sufficient to sustain a magnetic field which extracts the stored rotational energy in a collimated way; the transition to a dominant radio activity phase may be sufficiently abrupt to constitute a valid alternative to a CE. Accretion onto black holes of diffuse galactic gas conceivably fuels a section of $N(L, t)$ at low L evolving only on the longer time scales associated with the history of the interstellar medium (including recent additions from cooling inflows for the galaxies sitting in clusters; Cowie and Binney 1977); this fueling mode may accentuate the differential character of active galactic nucleus evolution up to a truly bimodal distribution. Perhaps the best model that involves large-scale conditions is the compact star cluster fueling a black hole, but replenished by events of galaxy merging as discussed by Roos 1981; a second time scale for the dimming is introduced by the hierarchical clustering of the groups where the merging rate is high, into rich clusters in which it tapers off (Carnevali, Cavaliere, and Santangelo 1981).

The conclusions of this paper are summarized as follows. The statistical framework to describe the populations dynamics of quasars and radio galaxies in the (L, t)-plane is conveniently based on the continuity equation for $N(L, t)$; the modes of energy release translate into the geometry of the characteristics of that equation, which determine the main course (density or luminosity evolution, uniform or differential) of the source statistics.

Primary energy sources that are gravitational and compact generate characteristics with effective time scales obeying $dt_s/dL \leq 0$, which drive population evolutions globally differential in L and sharply differential in t. A combination of an early density with a late luminosity evolution provides a simple and fitting first approximation for the overall run of the observed populations, independent of the uncertain details of the initial conditions; the emergence of the objects into recognizable and fully evolutionary quasar or radio galaxy regimes ought to occur at luminosities between 10^{-1} and 10^{-3} the maximum value. One specific model meeting many of these requirements is provided by sub-Eddington accretion onto a $M > 10^6\ M_\odot$ black hole from a giant, dense star cluster during its collisional self-destruction; the associated counts rise steeply at high fluxes and then converge rapidly, not unlike the behavior of the optical QSOs.

As for direct modeling of the data, these considerations open the perspective of using as a base in the (P, z)-plane, besides analytical continuations, also trial evolution functions of a form intrinsic to whole categories of physical processes for liberation of gravitational energy: scale-free power laws $\dot{L} \propto L^{1+p}$, or more structured $\dot{L} = f(L)$ modified by radiative efficiency, and containing a scale imprinted by imperfect coupling of the inner engine to its mass supply or by constraints to a black hole growth.

Useful and stimulating discussions with G. Setti, J. V. Wall, and R. Windhorst are gratefully acknowledged. We thank A. Franceschini, G. De Zotti, and G. C. Perola for comments and for critical reading. Suggestions by the referee improved the presentation of the paper. Work supported by C.N.R. and M.P.I.

APPENDIX

MODELS DESCRIBING THE RELEASE OF GRAVITATIONAL ENERGY

(summary: Table 1)

Class 1: Accretion onto a Black Hole

The active potential well is provided by an already formed black hole, and energy is released by mass inflow from an external supply towards the horizon; the requirement is $\dot{M} = 10^{-2}\eta^{-1}L_{45}\ M_\odot\ \mathrm{yr}^{-1}$, where η = overall efficiency.

Gas lost by stars throughout the body of a surrounding galaxy is easily dispersed by supernova-driven winds or ablated by ram pressure of an intercluster medium, before much of it gets into the nucleus (cf. Gisler 1976; Gunn 1979); its continuous inflow is likely to provide fuel only for a low-level, prolonged activity. Higher fueling rates are provided by the gas liberated from the stars in a giant cluster surrounding the nuclear black hole, when they are disrupted by tidal effects on passing by the hole, or, at even higher densities, when they collide between themselves (cf. Hills 1975; Frank 1978). Either way, the primary constraint—orbital kinetic energy of the single stars is dissipated rapidly in the unbinding and cooling of the resultant debris, which thus is allowed to fall further toward the hole. If the mass flows in with a small residual j (specific angular momentum), a quasi-spherical accretion flow may prevail (Rees 1978); otherwise, j will be removed in an accretion disk, which thickens by radiation pressure at high values of $\dot{M}$. When the inner engine works at very high regimes, $\dot{L}$ will be marked by the scale $L_E = 1.3 \times 10^{46} M_8$ ergs s^{-1}.

Pure tidal disruptions by a hole of mass $m\ M_\odot$ in a cluster core of radius R_{pc} pc comprising N stars of 1 $M_\odot$ can provide gaseous debris only at a rate $\dot{m}_t = 10^{-2} m_6^{4/3} R_{pc}^{-5/2} N_8^{1/2}$ limited by the conditions: $N_8 < R_{pc}$ if anelastic collisions between stars (discussed below) are not to dominate; and $m_6^{4/3} < 10 R_{pc}$ for the critical radius (entering

which the stars are doomed to disruption, Rees 1978) to remain inside the high-density core region. As the hole grows—faster than the core can contract—the power production increases at a rate

$$\dot{L} = AL^{p+1}\begin{cases} p = \frac{1}{4} \\ \tau_0 = \dfrac{1}{pAL_0{}^p} \sim 9 \times 10^8 m_{i6}{}^{-1/3} N_{i8}{}^{-1/2} R_{ipc}\ \text{yr} . \end{cases} \tag{A1}$$

The increase of L is limited, however, not only as for the rate governed by $\dot{m}_t$, but also as for the maximum value (under 10^{45} ergs s^{-1}); this is because a core expansion phase is bound to set in (Shapiro 1977; McMillan, Lightman and Cohn 1981) when the hole mass approaches 10% of that in core stars, at least if $N < 10^7$. On the other hand, core contraction by pure evaporation takes place only on a time scale much longer than the elastic relaxation, $t_{ev} \approx 50 t_R \sim 2 \times 10^{11} N_8{}^{1/2} R_{pc}{}^{3/2}$ yr. Thus, if $t_{ev} < H_0{}^{-1}$ is to hold, $N \ll 10^8$ is required, but then the total energy liberated is limited: $E \lesssim 10\%\ \eta Mc^2 \leq 10^{59}$ ergs.

More promising are initial conditions of such high density that disruptive collisions of core stars dominate right away: a short collision time $t_c < t_R$ requires $N_8/R_{pc} > 1$, the velocity dispersion being such that a typical impact unbinds the partners; the debris production rate by such impacts is $\dot{m}_c = 10^{-2}(N_8/R_{pc})^{7/2} N_8{}^{-1}\ \text{yr}^{-1}$ (Frank 1978). This increases up to a point when N decreases (McMillan, Lightman, and Cohn 1981), because a global virial equilibrium implies $-E \propto N^2/R \propto N^{-\beta}$, with $\beta = -1$ (whence $\langle v^2 \rangle = \text{const}$) when all of the debris loses all its kinetic energy and falls into the hole, and with $\beta \to 0$ (whence $\langle v^2 \rangle$ increases) otherwise. By disruptions and the attendant core contraction, N decreases at an ever increasing rate $\dot{N} \propto -N^{-(9+7\beta)/2}$ while, with no debris dispersion outward, the hole grows as

$$\dot{m} = -\dot{N} \propto [(N_i + m_i - m)/N_i]^{-(9+7\beta)/2} .$$

Now $\dot{m}_c$ is independent of the hole and can be very large; thus, if an appreciable fraction of that debris production can work its way down to the hole, a super-Eddington regime may prevail (McMillan, Lightman, and Cohn 1981): the condition $\dot{m}_c > L_E/c^2$ at given η may be recast into the form

$$m\left(\frac{N}{N_i}\right)^{(9+7\beta)/2} < 4.5 \times 10^5 \frac{\eta}{0.1}\left(\frac{N_{i8}}{R_{ipc}}\right)^{7/2} \frac{1}{N_{i8}} . \tag{A2}$$

Obviously satisfied for small initial m_i, it remains satisfied up to large masses when N_{i8}/R_{ipc} exceeds 1 considerably. The corresponding luminosity, bounded by the Eddington limit of the freely growing hole (Maraschi *et al.* 1979), increases up to $L_E(NM_\odot/2) \equiv \Lambda/2$ as given by

$$\dot{L} = a(\Lambda - L)^{-k}\begin{cases} k = (9+7\beta)/2; \quad \Lambda = 1.3 \times 10^{46}(N_{i8} + m_{i8}) \\ \tau = \dfrac{(\Lambda - L_0)^{k+1}}{\alpha(k+1)} \sim \dfrac{12}{11+7\beta} 10^9 \left(\dfrac{R_{ipc}}{N_{i8}}\right)^{7/2} N_{i8}{}^2\ \text{yr} . \end{cases} \tag{A3}$$

On the other hand, when N_{i8}/R_{ipc} is closer to unity and $N_{i8} > 1$ holds,[6] the regime is sub-Eddington upward of a mass $m > 10^6$–10^7, and the power increases following the scale-free dynamics of the supply:

$$\dot{L} = AL^{p+1}\begin{cases} p = \dfrac{11+7\beta}{9+7\beta} \\ \tau_0 = \dfrac{1}{ApL_0{}^p} \sim \dfrac{12}{11+7\beta} 10^9 \left(\dfrac{R_{ipc}}{N_{i8}}\right)^{7/2} N_{i8}{}^2\ \text{yr} . \end{cases} \tag{A4}$$

Since the hole grows at the expense of the self-gravitating core, $\dot{m}_c$ is bound to peak and start decreasing as soon as half of the mass has been engulfed (at $L_{max}/L_0 \sim 2^{(9+7\beta)/2}$), because then the hole dominates the dynamics of the core determining the orbits of the individual stars. From the debris production rate given by McMillan, Lightman, and Cohn 1981 we find that the output decreases following the approximate law

$$\dot{L} = -AL^{p+1}\begin{cases} p = \frac{1}{2} \\ \tau \sim \left(\dfrac{\eta}{0.1}\right)^{1/2} \dfrac{9}{2^{(9+7\beta)/4}} 10^9 \dfrac{R_{ipc}{}^{7/4} N_{i8}{}^{1/2}}{m_8{}^{1/4}} \left(\dfrac{R_{ipc}}{N_{i8}}\right)^{7/4} \text{yr} . \end{cases} \tag{A5}$$

With disruptive collisions, power and energetics are sufficient, in principle, for $L > 10^{45}$ ergs s^{-1} and $E > 10^{59}$ ergs; however, the fate of the debris is not assessed yet: less bound at production (Rees 1978), it is easily blown out near

[6] For values of N_{i8}/R_{ipc} close to 1, the lower limit for collisions to dominate, tidal disruptions still may play a role at $m \gtrsim 10^6$ but only within the narrow range $m_b/m_a \sim 6(R_{ipc}/N_{i8})^{3/2}$.

the Eddington limit and thus the maximum L and $\dot{L}$ and the overall energetics will decrease (McMillan, Lightman, and Cohn 1981); the same regime under unlimited accretion is also less effective in converting the mass actually accreted. In sum, the sub-Eddington regime (upward of $m \approx 10^6$) appears to be favored by higher efficiency at the hole and by less extreme densities in the star cluster.

All these simple models lack substantial anisotropy; they can describe more directly the optical QSOs, unpolarized and little variable. Sharp and persistent anisotropies associated with nonthermal output are indicated by a section of the data, concerning primarily the many radio jets, and, less directly, the OVV's and BL Lac objects. The angular momentum $\boldsymbol{J}$ of a massive object is a prime candidate to provide such an arrow in space, and rotation is the best converter of gravitational energy into low-entropy power.

Class 2: Rotating, Magnetized Configurations

The simplest high-$\boldsymbol{J}$ models obtain when mass supply, gravity source, and source of coherent angular momentum just coincide: a self-gravitating, rotating and magnetized plasma body (spinar, see Morrison and Cavaliere 1971; magnetoid, see Ginzburg and Ozernoy 1977 and references therein) that contracts gradually under control of its own $\boldsymbol{J}$, in the condition of large rotational energy W close to virial-like equilibrium, $2W + V \sim 0$ or $\Omega^2 R^3 \sim$ const.

The smaller the initial j_0 (but $j_0 > j_{\min} = GM/c$), the more compact and hence more powerful will be the resulting quasi-equilibrium configuration. Not only does the magnetic field, intensified during the contraction by flux (ϕ) conservation, provide internal coherence and some axial support (adding to any internal radiation pressure), but also its outward extensions set up a large-scale configuration of magnetic and induced or electrostatic electric fields, which extract angular momentum and rotational energy: $L = \Omega \dot{J}$ for an approximately rigid rotation. The rate

$$\dot{J} \sim -\frac{\phi_p}{c}\,\Omega \left(\frac{\Omega R}{c}\right)^{2m}$$

(see, e.g., Morrison and Cavaliere 1971) depends only on the polarity of the poloidal component of $\boldsymbol{B}$ ($m = 1$ corresponds to a dipolar structure, etc.); a component of $\boldsymbol{B}$ transverse to $\boldsymbol{J}$ is necessary, however, to redistribute within the body the stresses deriving from the braking processes (cf. Ozernoy and Usov 1973). The power is emitted in a mixture of Poynting flux and relativistic wind crossing the critical surface where the corotation velocity reaches the wave velocity, Alfvén or electromagnetic: $L \approx cR_c^2 B_c^2$.

Removal of J allows further gradual contraction at an ever increasing rate: $\dot{R} \propto -R^2 L$; the decreasing moment of inertia spins up the body, with an attendant luminosity increase $L/L_0 = (R/R_0)^{-(3+m)}$:

$$\dot{L} = AL^{p+1} \begin{cases} p = (2+m)/(3+m) < 1 \\ \tau_0 = \dfrac{1}{pAL_0{}^p} \sim 10^8 \left(\dfrac{\phi_p{}^2}{GM^2}\right)^{-1/4} M_8\, L_{42}{}^{-3/4}\ \text{yr} \qquad (m = 1)\ ; \end{cases} \tag{A6}$$

τ decreases subsequently after $\tau = \tau_0 (L_0/L)^p$.

A final dimming and a cutoff must be expected either by terminal collapse to a black hole configuration, or by loss of active flux. One instance of the latter effect has been treated by Ozernoy and Usov (1973): in a dipolar $\boldsymbol{B}$ configuration, for example, the magnetic axis tends to be aligned with $\boldsymbol{J}$ by the reaction of the braking torque, thereby decreasing the magnetic asymmetry relative to $\boldsymbol{J}$ responsible for the braking and the energy release. Thus the nonthermal L initially outshines an uncharacteristic thermal radiation, reaches a maximum at $L = L_{\max}$, say, but then undergoes a decrease described asymptotically by

$$\dot{L} = -AL\ , \qquad \tau = \frac{1}{ApL_{\max}{}^p \cos^2 \chi_i} = \frac{\tau(L_{\max})}{\cos^2 \chi_i}\ , \tag{A7}$$

where χ_i is the initial value of the angle of the magnetic axis to $\boldsymbol{J}$, ranging from $\sim 30°$ to nearly 90°.

In terms of the observed $P = \eta_r L$, the requirements are fixed by $B_4{}^2 M_8{}^2 = 0.3 \eta_r{}^{-1} P_{45}$, where η_r is the efficiency for conversion of large-scale electromagnetic power into radiation; the value of η_r, taking a hint from the Crab Nebula, may well approach 0.5. For all their designed efficiency in providing directly nonthermal forms of power, this class of models has been a constant source of concern about their stability. Although rotational instability and fragmentation are stabilized by the magnetic field and by any internal entropy, the lifetime in their highly active state has been evaluated at $\lesssim 10^7$ yr (Ozernoy and Usov 1973). These configurations are believed to end up in a massive hole over times $\lesssim 10^9$ yr (Ozernoy and Usov 1973; Begelman and Rees 1978).

Class 3: Accretion Flows onto Magnetized Rotators

The appealing features associated with high angular momentum (direct nonthermal output) and with accretion (long term stability enforced by a terminal collapsed configuration) are combined by a strongly magnetized accretion disk. Thin disk structures based on internal magnetic viscosity are relatively cold and still liable to instability (Rees 1978). Small-scale, external magnetic turbulence may generate interestingly hot, nonequilibrium coronae (Galeev,

Rosner, and Vaiana 1979; Liang 1979). Blandford (1976), however, has stressed that the large-scale components of $\boldsymbol{B}$ can be very efficient in electrodynamically removing $\boldsymbol{J}$ as in the spinar case, and extracting a power again or order $L_{45} \approx B_4{}^2 M_8{}^2$ in highly nonthermal form: Poynting flux and relativistic wind focused in the $\boldsymbol{J}$ direction (cf. Lovelace 1981). This model has been studied less so far, and here we confine ourselves to noting that self-consistency of the configuration requires the magnetic field to be related to the mass inflow by $B^2 \propto \dot{m}$ (Blandford 1976); with a tidal gas production, we find $L \propto B^2 m^2 \propto m^{10/3}$, and

$$\dot{L} \sim A L^{p+1} \begin{cases} p = 0.1 \\ \tau_0 \sim 7 \times 10^8 m_8{}^{-1/3} \text{ yr} . \end{cases} \tag{A8}$$

From a spinning hole surrounded by a magnetized accretion disk, rotational energy can be extracted in the form of a Poynting flux at a rate $L_{45} \approx 0.2 B_4{}^2 M_8{}^2 (J/J_{\max})^2$ (Blandford and Znajek 1977); on the other hand, the hole is efficiently spun up to $J/J_{\max} \lesssim 1$ when it accretes mass of such high j as to form a disk (Bardeen 1970). Rees *et al.* (1982) have recently stressed how such structures, when the accretion tapers off and the disk is thickened to a torus by dominant ion pressure, can best explain the observed conditions in the nuclei of radio galaxies: production of high-power jets, but of little optical radiation.

All the above models postulate comparable initial conditions: $10^8\ M_\odot$ or more, within 1 pc or less, that is, $\rho_0 \gtrsim 10^{-14}$ g cm^{-3}, with a limited amount of j. In the accretion models, the conditions are explicit. For spinar-like models, $j_0 < j_{\max} = G^{1/2} M^{2/3} \rho_0{}^{-1/6}$ is required for settling to a rotating, self-gravitating configuration that produces $L_0 \gtrsim 10^{43}$ ergs s^{-1}, implying $\tau_0 < 10^8$ yr (see details in Cavaliere, Morrison, and Wood 1971); then a density $\rho_0 \gtrsim 10^{-14}$ g cm^{-3} again results. This value is high on the scale of galactic densities, and little progress has been made to understand its origin, beyond conjecturing (see, e.g., Larson 1974; Shields and Wheeler 1978) a relation with events of protogalaxy formation and settling. Only for $j_0 < j_{\min}$ does one expect straight collapse to form and grow a massive black hole. When instead $j > j_{\min}$ holds (in fact, in a star cluster j is expected to be close to its statistical value $\gg j_{\min}$), then its amount and distribution steer the system (Begelman and Rees 1978) along a branched sequence of stages that may include spinar-like phases and should often end up in a terminal black hole.

On these events the current scenarios lose predictive power. Our approach will focus first on statistical features common to whole classes of such possible outcomes, then seek from finer fittings of the populations a clue to the stage most represented in the activity of galactic nuclei, and to any remaining imprint of its formation process.

REFERENCES

Avni, Y., and Tananbaum, H. 1982, *Ap. J. (Letters)*, **262**, L17.
Bardeen, J. M. 1970, *Nature*, **226**, 64.
Begelman, M. C., and Rees, M. J. 1978, *M.N.R.A.S.*, **185**, 847.
Blandford, R. D. 1976, *M.N.R.A.S.*, **176**, 465.
Blandford, R. D., and Rees, M. J. 1978, *Pittsburgh Conference on BL Lac Objects*, ed. A. M. Wolfe (Pittsburgh: University of Pittsburgh), p. 328.
Blandford, R. D., and Znajek, R. L. 1977, *M.N.R.A.S.*, **179**, 433.
Braccesi, A., Zitelli, V., Bònoli, F., and Formiggini, L. 1980, *Astr. Ap.*, **85**, 80.
Carnevali, P., Cavaliere, A., and Santangelo, P. 1981, *Ap. J.*, **249**, 449.
Cavaliere, A., Giallongo, E., Messina, A., and Vagnetti, F. 1982, *Astr. Ap.*, **114**, L1.
Cavaliere, A., Morrison, P., and Wood, K. 1971, *Ap. J.*, **170**, 223 (CMW).
Cavaliere, A., Danese, L., De Zotti, G., and Franceschini, A. 1981, *Astr. Ap.*, **97**, 269.
Cheney, J. E., and Rowan-Robinson, M. 1981, *M.N.R.A.S.*, **497**, 195.
Cowie, L. L., and Binney, J. 1977, *Ap. J.*, **215**, 723.
Danese, L., De Zotti, G., and Mandolesi, N. 1982, preprint.
Frank, J. 1978, *M.N.R.A.S.*, **184**, 87.
Galeev, A. A., Rosner, R., and Vaiana, G. S. 1979, *Ap. J.*, **229**, 318.
Ginzburg, V. L., and Ozernoy, L. M. 1977, *Ap. Space Sci.*, **50**, 23.
Gisler, G. R. 1976, *Astr. Ap.*, **51**, 137.
Gunn, J. E. 1979, in *Active Galactic Nuclei*, ed. C. Hazard and S. Mitton (Cambridge: Cambridge University Press), p. 213.
Hills, J. G. 1975, *Nature*, **254**, 295.
Kardashev, N. S. 1962, *Soviet Astr.*, **6**, 317.
Kellermann, K. I., and Pauliny-Toth, I. I. K. 1981, *Ann. Rev. Astr. Ap.*, **19**, 373.
Koo, D. C., and Kron, R. G. 1982, *Astr. Ap.*, **105**, 107.
Larson, R. B. 1974, *M.N.R.A.S.*, **166**, 585.
Layzer, D. 1976, *Ap. J.*, **206**, 559.
Liang, E. P. T. 1979, *Ap. J. (Letters)*, **231**, L111.
Longair, M. S. 1966, *M.N.R.A.S.*, **133**, 421.
Lovelace, R. V. E. 1981, in *Plasma Astrophysics* (Paris: ESA), SP-161, p. 215.
Maccacaro, T., Avni, Y., Gioia, I. M., Giommi, P., Liebert, J., Stocke, J., and Danziger, J. 1982, preprint.
Maraschi, L., Perola, G. C., Reina, C., and Treves, A. 1979, *Ap. J.*, **230**, 243.
Mathez, G. 1978, *Astr. Ap.*, **68**, 17.
McMillan, S. L. W., Lightman, A. P., and Cohn, H. 1981, *Ap. J.*, **251**, 436.
Morrison, P., and Cavaliere, A. 1971, in *Nuclei of Galaxies*, ed. J. K. O'Connell (Amsterdam: North-Holland), p. 485.
Neugebauer, G., Oke, J. B., Becklin, E. E., and Matthews, K. 1979, *Ap. J.*, **230**, 79.
Ozernoy, L. H., and Usov, V. V. 1973, *Ap. Space Sci.*, **25**, 149.
Peacock, J. A. 1982, *M.N.R.A.S.*, **199**, 987.
Peacock, J. A., and Gull, S. F. 1981, *M.N.R.A.S.*, **196**, 611.
Perola, G. C. 1981, *Fund. Cosmic Phys.*, **7**, 59.
Rees, M. J. 1978, *Phys. Scripta*, **17**, 193.
Rees, M. J., Begelman, M. C., and Blandford, R. D. 1980, preprint.
Rees, M. J., Begelman, M. C., Blandford, R. D., and Phinney, E. S. 1982, *Nature*, **295**, 17.
Roos, N. 1981, *Astr. Ap.*, **104**, 218.
Scheuer, P. A. G., and Readhead, A. C. S. 1979, *Nature*, **277**, 182.
Schmidt, M. 1978, *Phys. Scripta*, **17**, 329.
Schmidt, M., and Green, R. F. 1982, in *Astrophysical Cosmology*, ed. H. A. Brück, G. V. Coyne, and M. S. Longair (*Pont. Acad. Scientiarum Scripta Varia*, **48**, 281).
Setti, G., and Woltjer, L. 1982, in *Astrophysical Cosmology*, ed. H. A. Brück, G. V. Coyne, and M. S. Longair (*Pont. Acad. Scientiarum Scripta Varia*, **48**, 315).
Shapiro, S. L. 1977, *Ap. J.*, **217**, 281.

Shields, G. A., and Wheeler, J. C. 1978, *Ap. J.*, **222**, 667.
Turner, E. L. 1980, *Ap. J. (Letters)*, **242**, L135.
van der Laan, H., and Windhorst, R. A. 1982, in *Astrophysical Cosmology*, ed. H. A. Brück, G. V. Coyne, and M. S. Longair, (*Pont. Acad. Scientiarum Scripta Varia*, **48**, 349).
Wall, J., and Benn, C. 1982, in *IAU Symposium 97, Extragalactic Radio Sources*, ed. D. S. Heeschen and C. M. Wade (Dordrecht: Reidel), p. 441.
Wall, J. V., Pearson, T. J., and Longair, M. S. 1980, *M.N.R.A.S.*, **193**, 683.
———. 1981, *M.N.R.A.S.*, **196**, 597.
Woltjer, L. 1978, *Phys. Scripta*, **17**, 367.

A. CAVALIERE, E. GIALLONGO, and F. VAGNETTI: Istituto Astronomico c/o Istituto di Fisica, p. A. Moro 2, 00185 Roma, Italy

A. MESSINA: Istituto di Astronomia, via Zamboni 33, 40126 Bologna, Italy